

Comagnetometer probes of dark matter and new physics

W. A. Terrano and M. V. Romalis
Physics Department, Princeton University

We discuss the use of comagnetometry in studying new physics that couples to fermionic spin. Modern comagnetometry is – in absolute energy units – the most sensitive experimental technique for measuring the energy difference between quantum states, reaching sensitivities in the 10^{-26} eV range. The technique suppresses the magnetic interactions of the spins, making searches for non-standard-model interactions possible. Many implementations have been developed and optimized for various uses. New physics scenarios which can be probed with comagnetometers include: EDMs, violations of Lorentz invariance, Goldstone bosons of new high-energy symmetries, CP-violating long-range forces, and axionic dark matter. We consider the prospects for improvements in the technique, and show – based purely on signal-to-noise ratio with existing technology – that there is room for several orders of magnitude in further improvement. We also evaluate several sources of systematic error and instability that may limit improvements.

1. INTRODUCTION AND HISTORY OF THE FIELD

After the discovery of nuclear spins in 1933 [1] and the demonstration of control over them via their magnetic moments in 1938[2] – accomplishments earning the 1943 Nobel prize for Otto Stern and the 1944 Nobel prize for Isidor Rabi – nuclear magnetic resonance burgeoned as a technique in condensed matter and medical physics, beginning with the experiments of Bloch and Purcell[3, 4] in 1946 for which they shared the 1952 Nobel prize.

The use of nuclear spins for fundamental physics¹ – and with it the development of comagnetometry – did not occur until 1960 when Hughes[5] and Drever[6] compared the magnetic resonances of ${}^7\text{Li}$ and a proton at different orientations of the ${}^7\text{Li}$ quadrupole relative to the galactic center.

Comagnetometry is an essential technique when searching for new physics with spin-dependent couplings, as magnetic interactions dwarf the new physics signals by several orders of magnitude. The simplest nuclear-spin Hamiltonian for a system with total angular momentum \vec{F} is

$$(1) \quad \mathcal{H}_{\text{spin}} = \mathcal{H}_{\text{mag}} + \mathcal{H}_{\text{BSM}} + \dots = \vec{\mu}_N \cdot \vec{B} + \vec{\sigma}_N \cdot \vec{\beta} + \dots$$

with the additional terms depending on the specific comagnetometer implementation. Magnetic interactions \mathcal{H}_{mag} are described by the magnetic moment of the nucleus $\vec{\mu}_N = \mu \vec{F}/F$ and the magnetic field \vec{B} . Beyond-the-Standard-Model interactions are described by the spin moment of the nucleus $\vec{\sigma}_N = \vec{F}/F$ and an effective field $\vec{\beta}$ appropriate to the beyond-the-standard model coupling of interest – for instance, in an electric-dipole-moment search $\vec{\beta} = d_N \vec{E}$ with \vec{E} the applied electric field, and d_N the searched-for electric-dipole-moment. To extract \mathcal{H}_{BSM} from $\mathcal{H}_{\text{spin}}$ the experimentalist typically applies a characteristic time-dependence to $\vec{\beta}(t)$. Even so, fluctuations in \vec{B} must be suppressed to eliminate correlations – coincidental or systematic – between the time-dependences of $\vec{\beta}$ and \vec{B} . Comagnetometry achieves this by comparing spins with differing $\vec{\mu}$ or differing $\vec{\beta}$. Other experimental approaches to study similar BSM physics have been used as well, as summarized, for example, in a recent review[7].

Since the era of Hughes and Drever, comagnetometry has improved in absolute energy sensitivity by 12 orders of magnitude. Figure 1 shows the progress in measuring the energy difference between nuclear spins pointing one way or the other in absolute space. Comagnetometers built for other purposes[8, 9] have achieved energy sensitivities in the 10^{-26} eV range.

¹Ramsey did use bare neutrons for a neutron EDM measurement in 1951 that went unpublished until 1957, when the discovery of parity violation convinced them to publish their negative result.

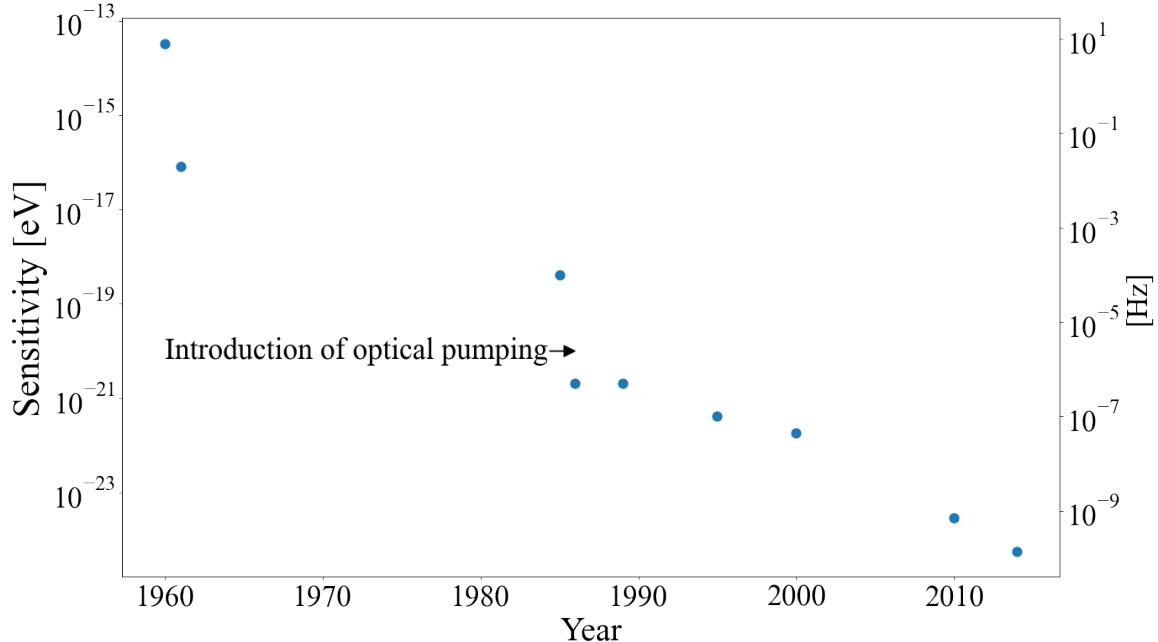


FIGURE 1. The progress in energy sensitivity of comagnetometers since Hughes and Drever. These results are for the energy of a spin due to its absolute orientation. The largest jumps in improvement came with the ability to create relatively pure ensemble quantum states of large numbers of nuclei via optical pumping in the 1980s, and with the implementation of advanced quantum magnetometers for the read-out systems in the 2000s. References, from top-left to bottom-right: [5, 6, 10, 11, 12, 13, 14, 15, 16]

2. COMAGNETOMETRY

The requirements of specific measurements have driven the development of a variety of comagnetometer implementations, with applications to angular-rotation sensing and fundamental physics. This section provides a brief description of some comagnetometers used in fundamental physics searches. This article – and only to limit the scope – focuses on comagnetometers that use at least one nuclear spin. This means neglecting important electron-spin comagnetometers such as those in electron EDM experiments that compare the energies of various electronic spin states[17, 18, 19, 20], and spin pendulums which compare the interactions of electronic spin and electronic orbital angular momentum[21, 22].

State-of-the-art comagnetometers all use optical pumping – in some fashion – to generate highly-non-thermal spin ensembles. Schematically, the technique is to transfer optical angular momentum from a laser to an electronic excited state by optical pumping, and then on to the nucleus. Depending on the transition energies of the atoms and available lasers, some nuclear hyper-fine states can be pumped directly while others are polarized via spin-exchange collisions with a more easily polarized atom.

2.1. General comagnetometer considerations. The main types of nuclear-spin comagnetometers are distinguished by: comparison type (energy splitting or quantization axis), spatial distribution (overlapping or not), the nuclear spin species studied, and the readout system used.

2.1.1. Comparison type: Clock vs quantization axis.

Clock comparisons: The precession frequency f of each spin ensemble i is measured, giving its

spin-up/spin-down energy splitting $\Delta E_{\text{spin}} = hf_i$. They are then combined in ratios or linear combinations which isolate \mathcal{H}_{BSM} as well as possible from \mathcal{H}_{mag} and other non-BSM contributions to $\mathcal{H}_{\text{spin}}$. Clock comparisons are mostly limited by state-dependent self-interactions of spins and by back-action of the read-out system on the nuclei, necessitating precise and repeatable initialization of the ensemble state and quantum decoupling techniques operating at the precision limit.

Quantization-axis comparisons: The quantization axes of two spin ensembles are compared to determine if there is a component of \mathcal{H}_{BSM} acting on one of the ensembles. These systems are largely limited by nano-radian instability in the read-out and polarization systems, which also affect the quantization axes, and by the trade-off between signal size and polarization lifetime.

2.1.2. Spatial distribution: overlapped vs separated.

Spatially-overlapped spins: The spin ensembles are contained in the same chamber, so that they nominally sample the same volume and the same \vec{B} . Since the ensembles are in the same chamber they must be of different species. Surface effects, gradients in temperature and gradients in polarization decay mean the volume coverage can never be precisely identical.

Spatially-separated spins: The spin ensembles are located in separate chambers. This allows the comparison of spins of the same type or of spins which require significantly different environments. Since they are not in the same volume they do not sample the same magnetic field, but using several cells allows drifts in both \vec{B} and gradients of \vec{B} to be canceled. If the same species is used in all chambers, $\vec{\beta}$ must be different in the different chambers.

2.1.3. Choice of Nucleus.

The nucleus must contain an unpaired nucleon to have net spin, and all comagnetometers to date have used isotopes with spin 1/2 or 3/2. The spin 3/2 nuclei have mass and charge quadrupoles allowing them to probe categories of interactions that are inaccessible to spin-1/2 nuclei, although the charge quadrupole couples to electric field gradients and shortens the spin ensemble coherence time. All competitive comagnetometers in recent decades have used either Mercury, or one of the three noble gases (helium, neon and xenon) that have stable isotopes of spin $\leq 3/2$ in reasonable abundance. Mercury can be pumped and probed directly with UV light, has a high vapor pressure at convenient temperatures and has remarkably long nuclear-spin lifetimes² and high-sensitivity to CP-violation due to its nuclear structure. Noble gases can have much higher densities than Hg vapors at room temperature. However at high densities they are polarized via fairly slow collisional-exchange-polarization techniques. The spin-polarization lifetime must be much longer than the polarization time to achieve highly coherent ensembles. This leads experimental attention naturally to the highly-inert noble gases; gases which form molecules de-polarize too quickly. Table 1 summarizes the most commonly used nuclei.

Isotope	Spin	Pumping	Phase
¹⁹⁹ Hg	1/2	optical	vapor
²⁰¹ Hg	3/2	optical	vapor
³ He	1/2	SEOP/MEOP	gas
²¹ Ne	3/2	SEOP	gas
¹²⁹ Xe	1/2	SEOP	gas
¹³¹ Xe	3/2	SEOP	gas

TABLE 1. Commonly used nuclei in comagnetometry. SEOP refers to spin-exchange-optical-pumping, where nuclear spin polarization is built up via collisions with an atom which can be optically pumped, typically potassium or rubidium. MEOP is metastability-exchange-optical-pumping, where a metastable state is optically pumped and then exchanged to the ground state during collisions.

²In the hundreds of seconds, corresponding to many collisions

2.1.4. Read-out system.

All read-out systems measure the magnetic moment of the nucleus. For Mercury, the same transitions used for polarization can be used to read-out the orientation of the nucleus by optical (Faraday) rotation of a linearly-polarized probe beam. Noble gas systems have proven effective both with optical magnetometry – via the same atoms used to polarize it – or with an external magnetometer connected to a pickup-loop near the cell. An internal magnetometer using alkali-metal atoms has the virtue of a good overlap between the magnetic sensor and nuclear spins. In addition, the effective magnetic field experienced by alkali-metal spins is enhanced due to contact interaction with nuclear spins by a factor ranging from 5 for helium to 500 for xenon[23, 24]. The tight-coupling of the internal read-out magnetometer results in back-action on the spins, which is the main drawback of the approach, along with its sensitivity to optical alignment. Decoupling and stabilizing the read-out also becomes complicated as the feedback or control pulses applied to the magnetometer affect the co-located nuclei as well. External magnetometers effectively minimize perturbations on the spins at the cost of difficulty in coupling it optimally to the spins while minimizing magnetometer noise.

2.2. Comagnetometer implementations for fundamental physics. In this section, we describe the general operating principles of some of the comagnetometers used for fundamental physics. Currently there are three leading implementations with roughly comparable energy resolution: The Hg-EDM comagnetometer (Sec. 2.2.1), the alkali-noble gas self-compensating comagnetometer (Sec. 2.2.3), and the He-Xe-SQUID clock-comparison (Sec. 2.2.2). Several creative implementations and measurements paved the way for these, which we touch on briefly. Some new concepts in comagnetometry which are under development are mentioned in “Future directions: Novel comagnetometers” (Sec. 4.2). The fundamental physics motivations, signatures and measurements are described in Section 3.

2.2.1. Mercury comagnetometers. The $^{199}\text{Hg} - ^{201}\text{Hg}$ comagnetometer, a spatially-overlapping clock-comparison, was developed in 1983[25] and was the first comagnetometer to utilize optical-pumping and optical-readout. The original apparatus was built to search for a dipole-dipole force between electrons and neutrons. Improved versions built in Seattle were used to search for preferred reference frames[11] and spin-gravity interactions[26].

The ^{199}Hg comagnetometer is unique in utilizing a single spin-species, so its design is completely intertwined with its application as an EDM search and it is discussed in the EDM section (Sec. 3.1). Since its first implementation in 1987 the EDM sensitivity has improved from 10^{-26} e-cm to $7 \cdot 10^{-30}$ e-cm [27, 28, 29, 30, 31, 9].

Mercury/Cesium comagnetometers – spatially-separated clock comparisons between the ^{199}Hg nucleus and the Cs electron – were first built in 1995[13]. A stack of three cells was used, with Hg in the outer two cells and Cs in the inner cell. This configuration avoids the quadrupolar ^{201}Hg nucleus and has been used to search for preferred frames[13, 32] and for long-range 5th forces[33, 34, 35].

2.2.2. Noble-gas/noble-gas clock-comparison. Clock comparisons between a pair of noble-gases date back to the 1980s when Chupp and collaborators implemented dual-species nuclear-spin-optical-pumping via spin-exchange with rubidium[36, 12], which underpins all other implementations. The first versions used a single chamber and alternated between a polarization period and a measurement period, with the measurement using NMR excitation and read-out techniques.

The $^3\text{He} - ^{129}\text{Xe}$ maser, a spatially-overlapping clock-comparison, was built in the 1990s[37, 38, 39] and used for EDM[40], 5th force[41] and preferred frame[14] searches. The maser involved two chambers, one to generate a population inversion via optical pumping of the spins, and the other providing the readout and the positive feedback to maintain the masing via pickup coils resonant to the two maser frequencies. The atoms diffused between the two chambers via a small tube.

The $^{129}\text{Xe}-^{131}\text{Xe}$ comagnetometer was built as a gyroscope and used to search for new forces[42]. The system was a spatially-overlapped clock comparison with rubidium vapor in the same cell as the xenon. Lasers pumped and probed the Rb, and thereby the Xe through the Rb-Xe interaction.

The most recent all-noble-gas comagnetometers were $^3\text{He}-^{129}\text{Xe}$ – SQUID systems[43, 44, 45, 16, 46, 47]. The noble gases were polarized in a separate Rb spin-exchange optical pumping station and then were transferred to an evacuated measurement chamber. The spins were monitored with a SQUID magnetometer that measured the total field produced by the gas cell. The precession frequencies of the two nuclei were separated and extracted in data analysis and then a \vec{B}_0 invariant frequency inferred:

$$(2) \quad \omega_{\text{inv}} = \omega_{\text{Xe}} - \omega_{\text{He}}(\gamma_{\text{Xe}}/\gamma_{\text{He}}),$$

where ω_i and γ_i are the frequency and gyromagnetic ratios of species $i = \text{He}, \text{Xe}$.

This technique is currently limited by the self-interactions of the nuclear spin-ensembles. Significant further improvement could be possible with improved quantum-control and decoupling techniques, as discussed in section 4.1.2.

2.2.3. Alkali-metal/noble-gas self-compensating comagnetometer. These comagnetometers compare the spin-quantization axes of colocated spin ensembles, one spin being an alkali-metal vapor and the other a noble gas (specifically K-He and Rb-Ne). They have been built in a variety of configurations and used to search for preferred reference frames and 5th forces. The principles behind these comagnetometers are given in several publications[48, 49]. The spins are polarized in-situ: a laser optically-pumpes the alkali-metal electron spins, which in turn pump the noble-gas nuclei via spin-exchange collisions. When the external magnetic field \vec{B}_0 – applied along the pump direction – matches the total field exerted by the nuclear spins on the alkali spins, the deflection of the quantization axis of the electrons relative to the pump-beam is determined only by the difference in the non-magnetic interactions of the electrons and nucleons. The cancelation of the external field is only effective at frequencies below the Larmor frequency of the nuclear spins, but in that regime the alkali atoms experience a small magnetic field, small enough in fact that broadening due to alkali-alkali spin-exchange collisions is eliminated, and the alkali-spin orientation can be measured very sensitively via the polarization rotation of a linear polarized probe beam. This read-out consists of measuring the projection of the alkali-spins along the probe beam axis, so mechanical changes in the relative alignment of the pump and probe beams can be an issue. Designs aiming to ameliorate this mechanical sensitivity are under development. Comagnetometers of this type have been used in searches for 5th forces[8, 50, 51] and preferred frames[15, 52], and are well- suited to dark matter direct detection[53, 54].

3. FUNDAMENTAL PHYSICS RESULTS

3.1. Electric Dipole Moment Measurements. Electric-dipole searches are among the most important precision tests of fundamental physics. An intrinsic electric dipole moment – which has yet to be observed in any system – must violate T and therefore CP-symmetry[55]. Searches for nuclear EDMs are motivated by two major outstanding questions in fundamental physics: the strong-CP problem and the baryogenesis question. The strong-CP problem arises from instanton anomalies that generically produce a CP-violating term in the presence of a non-zero quark mass[56]. This CP-violating term, whose coefficient (θ_{QCD}) is expected to be $\mathcal{O}(1)$, is measured to be less than 10^{-10} . Hence the problem. The baryogenesis question is: how did the universe come to contain more matter than anti-matter? Generating a matter/anti-matter asymmetry requires a process that simultaneously violates CP-symmetry, violates Baryon number conservation and is out of equilibrium[57]. No such process in the standard model is sufficiently strong, making the

identification of additional CP- violation an important part of understanding how the Universe came to be.

EDM measurements with nuclear-comagnetometers began in 1984 using ^{129}Xe [58] and shortly thereafter using ^{199}Hg [27], which has greater sensitivity to the strong-CP parameter at equivalent EDM sensitivities. Here we discuss only the most recent measurements using diamagnetic atoms; the field is rich and there are good recent reviews of EDM experiments[17].

The most recent ^{199}Hg search used 4 chambers, each containing a vapor of ^{199}Hg . Different electric fields were applied to the 4 chambers, allowing the experimenters to cancel fluctuations in the magnetic field and its linear and quadratic gradients while maintaining sensitivity to an EDM. The ^{199}Hg nuclei were polarized by optical-pumping, and the precession rate of the nuclei in each chamber was measured by optical rotation of a laser. The most recent measurement, the sixth published iteration, reached an EDM sensitivity of $7 \cdot 10^{-30} e\text{-cm}$ [9]³, setting the tightest constraints on θ_{QCD} and several other potential sources of CP-violation[9, 59]. The sensitivity was limited by the combination of magnetic field gradients and redistribution of the liquid ^{199}Hg droplets.

The most recent ^{129}Xe EDM searches were noble-gas clock-comparisons (Sec. 2.2.2) between ^3He and ^{129}Xe gases[46, 47]. The ^3He atoms should have a negligible EDM due to their small size[60] while the ^{129}Xe atoms could have a sizable EDM, depending on the high-energy origin of the CP-violation[61, 59, 17, 62, 63]. An electric field (\vec{E}) was applied to the cell and inverted every few minutes, so the nuclei experienced many \vec{E} states per cell filling. The ω_{inv} during each \vec{E} state was extracted, and then ω_{EDM} calculated by weighting by electric field and inverse-variance of ω_{inv} and taking the mean. The most sensitive result reached $1.4 \cdot 10^{-27} e\text{-cm}$ and was limited by slow drifts in ω_{inv} : the duration of each \vec{E} -state was chosen to be shorter than the ω_{inv} drifts to eliminate systematics due to the drifts, but this limited the interrogation time of each electric field stat. The drifts seemed to originate from interactions between the nuclei, see Sec. 4.1.2.

3.2. Searches for Preferred Frames. Hughes and Drever’s seminal work[5, 6], marked the first of many searches for preferred frames with spins, motivated by a variety of theoretical ideas including non-universal couplings of gravity and electricity&magnetism, Lorentz-violating scenarios and the observation that CPT-violation generates preferred frames that could couple to spin[64, 65, 66, 67, 68, 69, 70]. Searches for preferred-frames using nuclei with charge-quadrupole-moments (spin-3/2 and higher) test the Lorentz-invariance of Maxwell’s equations at much greater sensitivity than can be done with photons[65, 71, 11, 72, 73]. Since the preferred frame is presumably fixed in the galaxy, the sensitive axis of the experiment must be modulated relative to the galaxy. Most experiments fix their sensitive axis in the lab and use the rotation of the Earth to modulate its direction relative to the galaxy. Other experiments use a rotation stage to change the orientation of the sensitive axis[15, 52, 32].

Searches for preferred frames with the alkali/noble gas comagnetometers (Sec. 2.2.3) used a rotary platform to rotate the entire experiment and move the BSM signal to a higher frequency[15, 52]. This type of comagnetometer features great initial sensitivity but challenging long-term stability due to its sensitivity to drifts in the optical alignment. The K-He experiment reached a sensitivity of $3 \cdot 10^{-24} \text{ eV}$ (0.7 nHz) to a preferred spin-orientation, and the Rb-Ne experiment a sensitivity a few times larger for quadrupolar shifts. These experiments were limited by imperfections in the inversion of the sensitive axis. This becomes a systematic issue due to the gyroscopic effect of the rotation of the lab, which produces a frequency shift that depends on the angle of the sensitive axis relative to the Earth rotation axis.

A preferred frame search using the $^3\text{He} - ^{129}\text{Xe} - \text{SQUID}$ system (Sec. 2.2.2) was made using the rotation of the Earth to modulate the orientation of the sensitive axis relative to the Galactic center. They were limited by self-interaction induced drifts which they attempted to model and

³In the first paper[58], they set a limit of $1 \cdot 10^{-26} e\text{-cm}$ and pointed out the technique could potentially improve by 4 orders-of- magnitude.

separate from the sidereal signature of new physics[44, 16]. There is disagreement both about the specific physical origin of these drifts, and how successful they were at disentangling the drifts from the signal of new physics[74, 75, 76].

3.3. 5th Force. An ultra-low-mass, weakly interacting boson can generate a weak, macroscopic force. Such particles are widely predicted, and if the particle is a pseudoscalar it would couple to the axial-current Lagrangian $\mathcal{L}_{ax} = g_{a\bar{\psi}\psi}\partial_{\mu}a\bar{\psi}\gamma^{\mu}\gamma^5\psi$ and generate a new force that couples to spin. Such particles – variously referred to as axions or axion-like-particles – are produced as the pseudo-Goldstone bosons of new, high-energy symmetries, just as pions are the pseudo-Goldstone bosons produced by chiral symmetry breaking. The coupling of a pseudo-Goldstone boson to standard-model fermions is given by $g_p = C_f m_f / f_a$ where m_f is the mass of the fermion, f_a is the energy scale of the symmetry breaking and C_f is a dimensionless coupling constant expected to be order-one. If the broken symmetry is not exact, like chiral SU(2), the boson picks up a small mass $m_b = \Lambda^2 / f_a$ where Λ is the explicit symmetry breaking scale. The interaction mediated by the boson is suppressed at distances larger than the Yukawa length of the boson $\lambda = \hbar / (m_b c)$. Searches for new long-range spin-coupled forces are therefore a sensitive and general way to search for new hidden symmetries[77].

A pure pseudoscalar mediates a dipole-dipole interaction:

$$(3) \quad V_{dd} = \frac{g_p^2 \hbar^2}{16\pi m_1 m_2 c^2 r^3} \left[(\hat{\sigma}_1 \cdot \hat{\sigma}_2) \left(1 + \frac{r}{\lambda}\right) - 3(\hat{\sigma}_1 \cdot \hat{r})(\hat{\sigma}_2 \cdot \hat{r}) \left(1 + \frac{r}{\lambda} + \frac{r^2}{3\lambda^2}\right) \right] e^{-r/\lambda}.$$

Here, $\hat{\sigma}_{1,2}$ are the spins of the two particles, $m_{1,2}$ their masses, and \vec{r} the position vector between them. If the boson has a scalar coupling g_s it also mediates a CP-violating $\hat{\sigma} \cdot \hat{r}$ interaction (sometimes called a spin-mass interaction):

$$(4) \quad V_{md} = \frac{\hbar g_s g_p}{8\pi m_1 c} \left[(\hat{\sigma}_1 \cdot \hat{r}) \left(\frac{1}{r\lambda} + \frac{1}{r^2} \right) \right] e^{-r/\lambda}.$$

In 5th force searches, the comagnetometer acts as the detector, and a source of the new force is placed in the vicinity to modify the Hamiltonian of the comagnetometer spins. In searches for the dipole-dipole interaction (Eq. 3) the source must contain polarized spins. In searches for the monopole-dipole interaction (Eq. 4) the source must contain unpolarized matter. The energy-shift from the new force is typically modulated by varying the source distance or polarization.

Spin-mass interactions of nucleons have been studied since the 1960's, when a proton gravitational dipole moment was briefly claimed before being ruled out[78]. In comagnetometer searches for a new spin-mass force, some mass of large density is moved closer to and further from the comagnetometer, changing the magnitude of the interaction in Eq. 4 through its \vec{r} -dependence. Many spin-mass experiments using comagnetometers have been performed, optimized for various ranges[79, 26, 42, 45, 50].

Spin-spin interactions of neutrons were first studied using a $^{199}\text{Hg} - ^{201}\text{Hg}$ comagnetometer and the polarized electrons in nearby magnetized material[25]. The neutron-neutron coupling was first studied using the $^3\text{He} - ^{129}\text{Xe}$ maser. A chamber filled with high-polarization-density ^3He sourced the potential, and its polarization was inverted at regular intervals to flip the sign of the spin-spin interaction (Eq. 3)[41]. The best current limits come from a similar experiment performed with an alkali-noble gas comagnetometer (K-He) as the detector[8], which improved on the earlier constraint by 3-orders of magnitude to set a limit on anomalous nuclear spin-spin interactions to be 2×10^{-8} of their magnetic interactions.

The exchange of spin-1 bosons can generate a greater variety of potentials than given in Eqns. 3 and 4, in particular long-range and velocity dependent interactions[80, 81]. Searches for these interactions can be optimized with different source geometries and motions. For many Yukawa

lengths, the best source is the spin-polarization of the Earth and its large rotational velocity[34]. Using the Earth as a source requires special comagnetometer geometries, and the mercury/cesium comagnetometer is being optimized for this.

3.4. Dark Matter. Axions or axion-like-particles are well-motivated extensions to the standard model of particles, as described in section 3.3. In the following, “axion” refers to anything that couples to the axial-current, including all generic pseudo-Goldstone bosons, and “QCD axion” refers to an axion that also couples to the QCD anomaly, and can thereby solve the strong-CP problem. In addition to mediating new forces, axions would be produced in the early universe and make up some or all of the dark matter of the Universe. Axionic dark matter consistent with cosmology can have a vast range of masses, roughly from 10^{-22} eV to 10^2 eV in the simplest scenarios. Historically, dark matter axions which also solve the strong-CP problem have attracted the most attention, but many others have been proposed and there is no specific reason that the dark matter particles need to resolve other outstanding problems in particle physics.

The relevant coupling to the standard model is via the pseudo-scalar Lagrangian discussed in the previous section (Sec. 3.3), but with the dark matter halo of the galaxy as the source. The non-relativistic Hamiltonian is then[82, 83]

$$H_{\text{ax}} \sim g_{\text{p}} a_0 m_{\text{a}} \left(\sum_j \vec{v}_j \cdot \vec{\sigma}_\psi \cos \omega_j t \right),$$

where the summation is over modes j of the axion field. The nuclear-spin energy splitting is modulated at the axion frequencies $\omega_j = E_j/\hbar$, and

at the coherence time due changes in the interference among the modes, and by experimentally controllable changes in the fermion spin σ_ψ orientation. The magnitude of the signal is proportional to $a_0 m_{\text{a}}$, where a_0 is the amplitude of the axion wave at the time of the measurement. On average, $a_0 m_{\text{a}} = \sqrt{\rho_{\text{DM}}(\hbar c)^3}$ where ρ_{DM} is the local dark matter density.

Axions which solve the strong-CP problem also induce oscillating EDM moments in nuclei[?]; Axions that directly couple to gluon fields have an unavoidable contribution their mass which puts it out of the frequency range of existing comagnetometers[?]. Going to higher frequencies requires resonant (NMR) techniques or axion-photon searches. It is unclear precisely over which mass ranges each technique will be optimal, but it seems plausible that from 10^{-22} to 10^{-13} eV (10 nHz - 100Hz), the best strategies will be comagnetometer based.

Some dark-matter searches using comagnetometers have been performed[84, 85], although so far with energy resolution of around a few 10^{-19} eV, significantly worse than that of state-of-the-art comagnetometers which reach 10^{-26} eV. An axion search reaching an experimental sensitivity of 10^{-26} eV would be able to probe axion symmetry scales of 10^{11} GeV, assuming the coupling constant C_f defined in Section 3.3 is one. This level is beyond even the most aggressive constraints inferred from stellar cooling, and within an order-of-magnitude or two of the axion symmetry scales currently probed by ADMX[86].

4. FUTURE DIRECTIONS

4.1. Fundamental and practical limitations. State-of-the-art comagnetometers are the most sensitive measurements of the energy-difference between two quantum states, of any type, in terms of absolute energy sensitivity. Different implementations are limited by different sources of instability, which at this level are challenging and time-consuming to identify and find solutions to – especially when pushing against multiple sources of instability at the same time. However, these do seem to be practical rather than fundamental limitations, and the fundamental sensitivity of these systems leaves the potential for significant further improvement. Of course, precision measurements in the real world that are limited by fundamental noise are rare.

4.1.1. *Sensitivity and limitations of the ^{199}Hg comagnetometer.* The most recent ^{199}Hg measurement reached a final energy sensitivity of 22 pHz ($9 \cdot 10^{-26}$ eV), and resolution of 6.5 nHz from each 240 s measurement[9, 87]. This is a factor of 2-3 larger than the signal-to-noise, as computed from the photon-shot-noise. The excess was attributed to a combination of magnetic-field gradients and migration of the ^{199}Hg droplets, which affected the distribution of the polarized nuclei. Making cells which can support high-coherence times is to some degree black magic and much effort has gone into increasing the coherence times and working life of the cells. It is unknown if, and by how much, they may be further improved. The spin-lifetime in the best cells were 600-1000 seconds, with a test cell with natural Hg reached a coherence time of 1000 s[87]. If those coherence times could be matched in 4 cells, the integration time could be increased by a factor of $b = 3 \sim 5$ for an equivalent improvement in statistical sensitivity⁴. Significant further improvement could be achieved by slightly increasing the temperature of the cells to obtain higher ^{199}Hg density, provided that does not introduce new sources of leakage current, which can introduce magnetic fields correlated with reversal of the electric field in the cell[9].

4.1.2. *Sensitivity and limitations of noble-gas clock comparisons.* The intrinsic frequency resolution of a clock-comparison experiment is described by the Cramer-Rao lower bound (CRLB)[44]

$$(5) \quad \sigma_f^2 \geq \frac{12}{(2\pi)^2 (A/\rho)^2 T^3} C$$

where σ_f is the uncertainty in [Hz], A is the signal amplitude, ρ is the (white-noise) amplitude spectral density in $[A/\sqrt{\text{Hz}}]$, T is the observation time in [s] and C is a dimensionless parametrization of the signal decay⁵.

The signal amplitude A (in magnetic field units) can be written as $A = c_f \mu_0 M_n$, where $M_n = \mu_n n P$ is the nuclear magnetization, given by the product of the nuclear magnetic moment μ_n , nucleon density n and nuclear spin polarization P , and c_f is a dimensionless flux coupling factor that describes the magnetic field sensed by the pick-up coil. The frequency uncertainty σ_f can be related to the effective magnetic field sensitivity $\sigma_B = 2\pi\sigma_f/\gamma_n$. Combining these equations we obtain

$$\sigma_B^2 = \frac{2\rho^2}{T} \frac{6C}{(c_f \gamma_n \mu_0 M_n T)^2}.$$

The first factor $(2\rho^2)/T$ gives the uncertainty in magnetic field measurement for a time T using a magnetometer with field sensitivity ρ . The second factor on the order of $1/(\gamma_n \mu_0 M_n T)^2$ gives a dimensionless sensitivity gain factor due to nuclear spin precession that is proportional to the angle of nuclear spin precession in their own magnetization.

A fundamental factor that can limit the sensitivity is the spin-projection-noise which is given for spin-1/2 systems by[88]

$$(\sigma_f^{\text{SN}})^2 = \frac{C_{\text{SN}}}{(2\pi)^2 N T_2 T}$$

where T_2 is the decay time, N the number spins and C_{SN} a constant of order 5-10 that depends on the experimental protocol. Unlike alkali-metal magnetometers, nuclear spin magnetometers are usually not limited by this source since they contain 10^{19} or more atoms. In the scenarios considered here the projection-noise limit is below the Cramer-Rao lower bound in all cases⁶.

Table 4 shows parameter values from the most recent $^3\text{He} - ^{129}\text{Xe} - \text{SQUID}$ measurement. The measurement time T_{Meas} in that experiment was chosen such that $T_{\text{Meas}} \times \text{Drift} \approx \sigma_f$. However, if the drifts were small enough that the measurement time could last the decay time, the Cramer-Rao

⁴Assuming the ratio of light and dark times remains constant. So far laser-related systematics have been below the statistical noise but they are a source of concern.[87]

⁵ $C=1$ for a constant signal, and $C=1.7$ for a signal that decays exponentially for one decay time.

⁶The speculative case is within a factor of a few of the projection-noise limit.

bound would drop an order of magnitude. This would require a reduction in the drifts by three-orders-of-magnitude. The drifts seem to be caused by interactions among the nuclei[76]; we provide more detail on those around Eq. 6 and in the discussion following outline other potential sources of instability. Table 4 also gives some near-term and long-term possibilities. The first two upgrades are realistic targets for near-term improvements, while the last three are technically challenging – although all levels have been reached in dedicated R&D setups.

In the real-world, precision experiments are typically limited by environmental noise and systematics. Some general considerations on likely issues are also covered below. In fact it may not be possible to reach best-ever levels on all parameters simultaneously as there are often trade-offs among them– in particular T_{Decay} is sensitive to the environment in many ways. Still, based only on signal-to-noise considerations the Cramer-Rao bound can be reduced tremendously, from what is already within a factor of 10 of the most sensitive nuclear spin measurements ever, the ^{199}Hg comagnetometer[9] and the stationary self-compensating comagnetometer[8].

System	Cell Mag [fT]	Coupling [geom.]	Readout [fT/ $\sqrt{\text{Hz}}$]	Self Int. [supp.]	T_{Decay} [s]	T_{Int} [s]	CRLB (σ_f) [nHz]
HeXe-2019	1.3×10^6	4.4×10^{-3}	6	1.5×10^{-3}	8000	500	2.7^a
Near-Term Targets: evolutionary progress							
Suppress Int	1.3×10^6	4.4×10^{-3}	6	3×10^{-6}	8000	8000	0.17
Geometry	1.3×10^6	0.22	1	1×10^{-7}	8000	8000	6×10^{-3}
Long-Term Potential: modified protocols needed							
Best Noise	1.3×10^6	0.22	0.1	1×10^{-8}	8000	8000	6×10^{-4}
Long Decay	1.3×10^6	0.22	0.1	3×10^{-9}	18000	18000	1.7×10^{-4}
High Pol ^b	4×10^7	0.22	0.1	4×10^{-12}	18000	18000	6.3×10^{-6}

TABLE 2. Experimental parameters of the 2019 Xe-EDM experiment[47] and possible avenues of improvements. Specific implementations needed to reach these levels are given in Table 4 in the appendix. “Cell Mag”: The magnetic field at the surface of the cell for the limiting species. “Coupling”: The ratio of field at the cell to field through the pick-up loop, which depends on the geometry of the system. “Readout”: The noise in the read-out sensor. This is usually dominated by the magnetic noise of the local environment. “Self Int.”: The factor by which the self-interaction Hamiltonian (Eq. 6) must be suppressed, by cancelling terms against each other, preparing the system with very small longitudinal component or decoupling the Hamiltonian. “ T_{Decay} ”: The decay time-constant of the transverse amplitude^c. “ T_{Int} ” Measurement time for a single frequency extraction. Taken to be T_{Decay} unless comagnetometer instabilities require shorter durations. “CRLB”: The theoretical best resolution of the experiment, computed for a single T_{Decay} time.

^aThe experimentally measured uncertainty was 3nHz.

^bGenerating high polarizations of both species simultaneously would require separate pumping cells or advancements in dual-species hybrid pumping, as the optimal pumping conditions for high Xe and high He densities are quite different.

^c $A(t) = A_0 e^{-t/T_{\text{Decay}}}$

It is not possible to predict whether all instabilities can be controlled well enough to reach the Cramer-Rao bound: we do not even know all the effects that may be important. We highlight some likely sources of instability and what it might take to control them.

- *Longitudinal interactions*: The drifts in current experiments are caused by cross-interactions of the nuclei, described by state-dependent Hamiltonians

$$(6) \quad \mathcal{H}_i = \sum_j \mu_0 \alpha_{ij} \vec{\mu}_i \cdot \vec{\mu}_j$$

where the $\vec{\mu}_{i,j}$ are the magnetic moments of nuclear spin species i, j , and the components of α_{ij} are coupling strengths on the order of 10^{-2} . All components of α_{ij} are generically non-zero and not canceled in the comagnetometer frequency. The $i = j$ terms depend on the cell geometry.

This Hamiltonian changes the spin-up/down energy splitting if there is a non-zero component of either nuclear spin along \vec{B} , and causes a frequency drift as this “longitudinal” component of the polarization decays away[89, 76]. The drift can be suppressed by precise state initialization to ensure there is no longitudinal polarization, specially chosen cell geometries[89, 76] and decoupling sequences[90]. The suppression required can scale faster than the SNR improvement, however.⁷ The improvements outlined in “Near-Term Targets” of Table 4 require suppressing self-interactions by $\mathcal{O}(10^4)$ compared to current experiments. Achieving the “Long-Term Potential” would require significantly greater control over the self-interacting portion of the Hamiltonian, especially if the cell magnetizations are increased.

- *Earth rotation effects:* The nuclei precess in the non-inertial frame of the rotating Earth so they pick-up an apparent frequency shift of $f_{\oplus} \sim 10 \mu\text{Hz}$ for a horizontal magnetic field at mid-latitudes[43]. This shift depends on the angle between the magnetic field and the Earth’s rotation axis, so anything that changes that angle also changes ω_{int} . Some specific potential issues are: tilts or twists of the apparatus from loading in the vicinity; changes in the background magnetic field; and changes in the orientation of the Earth’s rotational axis. Changes in the Earth’s rotation axis, known from very long baseline interferometry and observed in ring- laser gyroscopes are irreducible, and in a typical experimental configuration (mid-latitude & horizontal holding field) would contribute daily fluctuations of $\sim 0.5 \text{pHz}$ [91]. If the holding field is aligned with the Earth’s rotation axis[26] these are suppressed to tolerable levels (Table 5). Secular changes in the Earth’s rotation period correspond 0.1pHz changes in ω_{inv} as the Earth’s rotation period itself changes. These slow changes in Earth’s rotation can be monitored and removed easily by stellar observations[92, 93].
- *Gyroscopic coupling to lab motions:* Slow tilts of the lab due to tidal, atmospheric and local loading can produce a rotation around the sensitive axis of the system, which would be picked up by the same gyroscopic coupling that produces the Earth rotation effect (above). Commercial tilt-meters have a sensitivity around $7 \text{ nrad}/\sqrt{\text{Hz}}$ [94], a few times the resolution needed to monitor and subtract this coupling in the most sensitive scenarios. The success of ring-laser gyroscopes which are sensitive to twists demonstrates that – when much care is taken and the apparatus affixed to the bedrock – laboratory twists can be suppressed to around these levels[91].
- *Transverse self-interactions:* Since the cell is not spherical, there will be through-space Ramsey-Bloch-Siegert shifts of the nuclei on each other[16] caused by the magnetic field

⁷Imagine improving some aspect of the experiment by a multiplicative factor of b . How much do longitudinal interactions need to be suppressed to take full advantage? If the improvement is in the noise (or in signal, if achieved through better spin-SQUID coupling), the longitudinal interactions must be suppressed by $1/b$ to maintain the same integration time. If the increase is in the number of spins – through higher pressures or polarization fraction or both – the longitudinal interactions must be suppressed by $1/b^2$, as the higher polarization increases both the output signal and the internal magnetizations that source the longitudinal self-interactions. If the increase is in T_{Decay} , the longitudinal interactions must be suppressed by $1/b^{3/2}$ to take full advantage of the longer potential integration time. If T_{Int} increases relative to T_{Decay} the required suppression scales as $1/b^{5/2}$ (in the $T_{\text{Int}} \ll T_{\text{Decay}}$ limit) since more of the longitudinal magnetization decays.

of the rotating (transverse) component of the nuclear polarization. The signal sizes in the HeXe-2019 system should cause a transverse-magnetization-dependent frequency shift of ~ 500 pHz and scale quadratically with magnetization[76]. Since the rotating amplitudes are measured during data-taking this effect may be possible to account for metrologically.

4.1.3. *Sensitivity and limitations of Alkali-Noble gas self-compensating comagnetometers.* Alkali-Noble gas comagnetometers face three major sources of noise, so the limiting factor depends on the frequency and the measurement of interest: at low-frequency, fluctuations in the beam alignment; at high-frequency, the breakdown of the magnetic-field compensation; if there is any room in the middle, probe beam noise. Experiments which require mechanical motion of the comagnetometer or source masses are often limited by beam-alignment across the middle frequencies.

The most sensitive comagnetometer ever operated was a K- ^3He co-magnetometer used to search for spin-spin 5th forces, which reached an integrated sensitivity of 20 pHz (7×10^{-26} eV), with a noise level of 21 nHz/ $\sqrt{\text{Hz}}$ at the signal frequency of 0.3 Hz. This experiment was limited by laser intensity fluctuations within a factor of two of the shot noise limit, and within a factor of 5 of the best-ever alkali-metal magnetometer sensitivity[95].

Beam-alignment fluctuations and magnetic field noise both improve at higher frequencies, so a system with larger magnetization which can operate at higher-frequencies could be more sensitive. The effect of mechanical motion can be reduced with pulsed operation of the pump laser followed by measurements of the transient response of the coupled spin system. Unlike nuclear spin precession magnetometers, the self-compensating magnetometer measures the twist on the nuclei at static equilibrium and so does not have the gain factor due to measuring the precession frequency given by $\gamma\mu_0 M_n T$. Thus its sensitivity is limited by the best available sensitivity of the alkali-metal magnetometer.

4.2. **Novel comagnetometer implementations.** New ideas in comagnetometry are constantly being investigated, aiming for reduced sensitivity to various sources of systematic error. Here we give a brief description of some recent efforts, which explore several interesting avenues.

- $^3\text{He} - ^{129}\text{Xe}/^{21}\text{Ne}$ with Rb readout[96, 97, 89]: This system suppresses the longitudinal interactions that limit other Noble-gas comagnetometers by using the same volume for pumping and probing, permitting greater refinement and repeatability of the state initialization at the beginning of the probe time. It also increases the signal due to the contact interaction between Rb and nuclear spins. The read-out of the spin-precession is done via the Rb in the cell, meaning Rb-nuclear spin back-action must be decoupled. This is done using RF-pulses to rapidly invert the Rb orientation so it has no net longitudinal polarization. These pulses also mean the Rb sees no net magnetic field, allowing them to operate without spin-exchange relaxation even at the higher magnetic fields needed for noble gas NMR. The decoupling pulses themselves produce a species dependent frequency shift – much smaller than that of the Rb which they decouple but still much larger than the target sensitivity. This requires further decoupling, or operating in the dark with no pulses. Interactions between Rb and ^{21}Ne are ~ 15 times smaller than between Rb and ^{129}Xe , allowing longer spin-precession times and smaller Rb back-action, at the cost of dealing with ^{21}Ne quadrupolar effects. Current data shows the ^{21}Ne quadrupolar frequency splitting is smaller than the ^{21}Ne linewidth, even with decay times of several thousand seconds.
- *Transversely pumped* $^{129}\text{Xe} - ^{131}\text{Xe}$ [98, 99, 100]: This system suppresses the longitudinal-interactions that limit other Noble-gas comagnetometers by pumping the nuclei transversely to the holding field. To keep the transverse Rb aligned with the optics, the magnetic “holding” field is made up of pulses, with each pulse flipping the Rb by 2π . Generating a net Rb polarization along the xenon as the xenon rotate was implemented by reversing the laser polarization at the xenon frequencies or by modulating the magnetic holding field so

the xenon precession is slower when it is aligned with the beam and faster when it is anti-aligned. The pump/probe geometry permits feedback to reduce the build up of longitudinal polarization.

- **Dual Xe isotope spin maser**[101]: This approach uses a Rb magnetometer to apply positive feedback so the nuclear spins precess indefinitely with continuous optical pumping. Compared to earlier work on spin masers [28,13], this approach can be operated at a lower bias field because it does not rely on inductive detection of spin precession with a pick-up coil. Even though the spins precess indefinitely due to the positive feedback, the sensitivity of spin masers is still given by the Cramer-Rao bound with T equal to the spin coherence time. At longer times the feedback system introduces a random frequency walk due to coupling of the detection noise.
- **Comolecular comagnetometer**[102, 85]: This system compares the $^{13}\text{C} - ^1\text{H}$ of liquid state $^{13}\text{CH}_3\text{CN}$ molecules to improve the degree of spatial overlap between the comagnetometer spin-ensembles. These experiments used the classic NMR technique of polarizing the nuclei in a large magnetic field. The lack of hyper-polarization means the energy resolution of the first iteration was around $100 \mu\text{Hz}$ with 30 days of integration time. There is hope that hyper-polarization may be applied to this system[85].
- **Comagnetometer networks**: Searches for transient anomolous fields are motivated by astrophysical models predicting things such as domain walls, axion vortices or self-gravitating axion clusters, and more generally are just a good way to look for the unexpected[103, 104]. Identifying transients with a single comagnetometer is essentially impossible, as it would be indistinguishable from an experimental glitch. A network of comagnetometers looking for correlated glitches across the globe, however, has a chance of observing such a transient[104].

4.3. Potential Physics Reach. Real physics experiments are limited by systematics, so projections of physics reach are inherently speculative. However to give the reader an idea of what could be done, Table 3 shows rough sensitivities to the axion-decay-constant and ^{129}Xe EDM if the sensitivities outlined in Table 4 are reached, and control of systematics keeps pace. The “Near-term” scenario corresponds to line 3 of Table 4 and involves canceling drifts and optimizing the experimental geometry. “Optimistic” scenario corresponds to line 5 of Table 4, and requires matching the best readout noise yet achieved in such a system as well as the longest polarization lifetimes. “Speculative” scenario matches the highest spin-polarizations ever achieved, which have not yet been demonstrated in dual-species systems, along with vastly greater control over internal interactions due to the higher magnetizations. It may also be possible to improve the readout of the system even further – which could be a more profitable approach, although just as speculative.

Experimental progress	Integrated energy resolution [eV (Hz)]	Dark-matter-axion scale F_a/C_n [GeV]	Xe EDM [e-cm]
Near-Term	1×10^{-27} (2.5×10^{-13})	9.6×10^{11}	2.9×10^{-30}
Optimistic	4×10^{-29} (9.4×10^{-15})	2.6×10^{13}	1.1×10^{-31}
Speculative	1.4×10^{-30} (3.4×10^{-16})	7.1×10^{14}	4×10^{-33}

TABLE 3. Physics reach of a ${}^3\text{He} - {}^{129}\text{Xe} - \text{SQUID}$ system under conservative, optimistic and speculative scenarios, assuming 100 days of measurement. “Integrated Energy Resolution”: The uncertainty on $\hbar\omega_{\text{inv}}$. “Dark-matter-axion scale”: F_a is the symmetry-breaking scale of the axion (axion decay constant), C_n is a dimensionless coupling constant to nucleons, assumed to be order one. These limits apply specifically to axions with oscillation frequency below the repetition rate of the experiment, around 10^{-19} eV “Xe EDM [e-cm]”: The EDM measurements assume 25-33 kV voltage difference across the cell (5 kV/cm electric fields) with 5 high voltage states per decay time. Leakage current effects are largely canceled by the comagnetometer, with best measurements showing an effect of $\leq 1.77 \mu\text{Hz}/\mu\text{A}$, implying leakage current requirements of 3.9×10^4 , 110 and 40 fA respectively, although this may turn out to be an over-estimate. The most recent ${}^{199}\text{Hg}$ measurements measured steady-state leakage currents of 40 fA.

The sensitivities outlined in Table 3 are ambitious, and will require significant advances in the understanding of and the control over instabilities in this type of comagnetometer. They are, however, consistent with existing signal-to-noise ratios, which are phenomenal thanks to decades of work.

Enticingly, based on these estimates (and with more hard work and good fortune) a comagnetometer could come within nearly an order-of-magnitude of some heretofore almost unimaginable targets: axion dark matter produced by symmetry-breaking at the Grand Unification scale of 10^{16} GeV, and the standard-model prediction for the ${}^{129}\text{Xe}$ EDM of 5×10^{-35} e – cm[17]. If all goes well on the comagnetometry side, and another order-of-magnitude beyond Table 3 is to be achieved, the next technological break-throughs – whether in low-noise-materials, two-stage readout or elsewhere – may be driven by these fundamental physics motivations.

Acknowledgements: This work was made possible by Princeton University and the Simons Foundation

APPENDIX A. PHYSICAL PARAMETERS OF POTENTIAL UPGRADES

System	Dimensions [cm]			Xenon		Helium	
	Cell	Pickup	Cell-SQUID	P	pol	P	pol
	Diam.	Diam.	Z	[bar]	[]	[bar]	[]
HeXe-2019	2.0	0.24	2.9	0.14	0.12	0.65	0.004
Near-Term Targets: evolutionary progress							
Suppress Int	2.0	0.24	2.9	0.14	0.12	0.65	0.004
Geometry	5.0	1.4	4.1	0.14	0.12	0.65	0.004
Long-Term Potential: modified protocols needed							
Best Noise	6.7	5.0	4.7	0.14	0.12	0.65	0.004
Long Decay	6.7	5.0	4.7	0.14	0.12	0.65	0.004
High Pol	6.7	5.0	4.7	1.0	0.5	1.1	0.06

TABLE 4. Experimental parameters of the 2019 Xe-EDM experiment[47] and possible future improvements. All parameters have been demonstrated, albeit not necessarily in a comagnetometer system. “Cell-SQUID” is the distance from the center of the cell to the center of the SQUID pickup loop. “P” and “pol” are the pressure and polarization fraction of each noble gas species.

APPENDIX B. REQUIREMENTS ON STABILITY AND MONITORING

Progression	Typical B0			Polar B0		
	Earth Axis [fraction of]	B \perp [fT]	B0 Tilt [μ rad]	Earth Axis [fraction of]	B \perp [fT]	B0 Tilt [μ rad]
Near-Term	0.4	3×10^3	1	220	1×10^7	5×10^3
Optimistic	1.5×10^{-2}	78	2.6×10^{-2}	8	3×10^5	1.5×10^2
Speculative	5.4×10^{-4}	2.7	1×10^{-3}	0.3	1×10^4	5

TABLE 5. Stability requirements so that associated frequency shifts from changes in the gyroscopic pickup of Earth’s rotation remain below the statistical sensitivity. “Typical B0” are the requirements for a convenient mid-latitude, horizontally aligned magnetic field. “Polar B0” are the requirements if the magnetic field is aligned with the Earth’s rotation axis to within 100μ rad. “Earth Axis” is the changing orientation of the rotation axis of the earth. This is unavoidable and must be subtracted from the measured frequencies based on other observations and geophysical models. This column gives the maximum allowable fractional error in the model of the polar motion at the experiment site. “B \perp ” gives the requirement on how well known the transverse fields at the cell must be known, per measurement point and assuming a 2μ T holding field. “B0 Tilt” gives the requirement on how well tilts along the B0 axis must be known.

REFERENCES

- [1] I. Estermann, R. Frisch, and O. Stern. Magnetic moment of the proton. *Nature*, 132(3326):169–170, Jul 1933.
- [2] I. I. Rabi, J. R. Zacharias, S. Millman, and P. Kusch. A new method of measuring nuclear magnetic moment. *Phys. Rev.*, 53:318–318, Feb 1938.
- [3] F. Bloch, W. W. Hansen, and M. Packard. The nuclear induction experiment. *Phys. Rev.*, 70:474–485, Oct 1946.
- [4] E. M. Purcell, R. V. Pound, and N. Bloembergen. Nuclear magnetic resonance absorption in hydrogen gas. *Phys. Rev.*, 70:986–987, Dec 1946.
- [5] V. W. Hughes, H. G. Robinson, and V. Beltran-Lopez. Upper limit for the anisotropy of inertial mass from nuclear resonance experiments. *Phys. Rev. Lett.*, 4:342–344, Apr 1960.
- [6] R. W. P. Drever. A search for anisotropy of inertial mass using a free precession technique. *The Philosophical Magazine: A Journal of Theoretical Experimental and Applied Physics*, 6(65):683–687, 1961.
- [7] M. S. Safronova, D. Budker, D. DeMille, D. F. J. Kimball, A. Derevianko, et al. Search for new physics with atoms and molecules. *Rev. Mod. Phys.*, 90:025008, Jun 2018.
- [8] G. Vasilakis, J. M. Brown, T. W. Kornack, and M. V. Romalis. Limits on New Long Range Nuclear Spin-Dependent Forces Set with a K-He3 Comagnetometer. *Physical Review Letters*, 103(26):261801, December 2009.
- [9] B. Graner, Y. Chen, E. G. Lindahl, and B. R. Heckel. Reduced limit on the permanent electric dipole moment of ^{199}Hg . *Phys. Rev. Lett.*, 116:161601, Apr 2016.
- [10] J. D. Prestage, J. J. Bollinger, Wayne M. Itano, and D. J. Wineland. Limits for spatial anisotropy by use of nuclear-spin-polarized $^9\text{Be}^+$ ions. *Phys. Rev. Lett.*, 54:2387–2390, Jun 1985.
- [11] S. K. Lamoreaux, J. P. Jacobs, B. R. Heckel, F. J. Raab, and E. N. Fortson. New limits on spatial anisotropy from optically-pumped sup201hg and ^{199}Hg . *Phys. Rev. Lett.*, 57:3125–3128, Dec 1986.
- [12] T. E. Chupp, R. J. Hoare, R. A. Loveman, E. R. Oteiza, J. M. Richardson, et al. Results of a new test of local lorentz invariance: A search for mass anisotropy in ^{21}Ne . *Phys. Rev. Lett.*, 63:1541–1545, Oct 1989.
- [13] C. J. Berglund, L. R. Hunter, D. Krause, Jr., E. O. Prigge, M. S. Ronfeldt, et al. New limits on local lorentz invariance from hg and cs magnetometers. *Phys. Rev. Lett.*, 75:1879–1882, Sep 1995.
- [14] D. Bear, R. E. Stoner, R. L. Walsworth, V. Alan Kostelecký, and Charles D. Lane. Limit on lorentz and cpt violation of the neutron using a two-species noble-gas maser. *Phys. Rev. Lett.*, 85:5038–5041, Dec 2000.
- [15] J. M. Brown, S. J. Smullin, T. W. Kornack, and M. V. Romalis. New Limit on Lorentz- and CPT-Violating Neutron Spin Interactions. *Physical Review Letters*, 105(15):151604, October 2010.
- [16] F. Allmendinger, W. Heil, S. Karpuk, W. Kilian, A. Scharth, et al. New limit on lorentz-invariance- and cpt-violating neutron spin interactions using a free-spin-precession ^3He - ^{129}Xe comagnetometer. *Phys. Rev. Lett.*, 112:110801, Mar 2014.
- [17] T. E. Chupp, P. Fierlinger, M. J. Ramsey-Musolf, and J. T. Singh. Electric dipole moments of atoms, molecules, nuclei, and particles. *Rev. Mod. Phys.*, 91:015001, Jan 2019.
- [18] J. Baron, W. C. Campbell, D. DeMille, J. M. Doyle, G. Gabrielse, et al. Order of magnitude smaller limit on the electric dipole moment of the electron. *Science*, 343(6168):269–272, 2014.
- [19] W. B. Cairncross, D. N. Gresh, M. Grau, K. C. Cossel, T. S. Roussy, et al. Precision measurement of the electron’s electric dipole moment using trapped molecular ions. *Phys. Rev. Lett.*, 119:153001, Oct 2017.
- [20] ACME Collaboration, V. Andreev, D. G. Ang, D. DeMille, J. M. Doyle, et al. Improved limit on the electric dipole moment of the electron. *Nature*, 562(7727):355–360, October 2018.
- [21] B. R. Heckel, E. G. Adelberger, C. E. Cramer, T. S. Cook, S. Schlamminger, et al. Preferred-frame and CP-violation tests with polarized electrons. *Phys. Rev. D*, 78(9):092006, November 2008.
- [22] W. A. Terrano, E. G. Adelberger, J. G. Lee, and B. R. Heckel. Short-Range, Spin-Dependent Interactions of Electrons: A Probe for Exotic Pseudo-Goldstone Bosons. *Physical Review Letters*, 115(20):201801, November 2015.
- [23] S. R. Schaefer, G. D. Cates, Ting-Ray Chien, D. Gonatas, W. Happer, et al. Frequency shifts of the magnetic-resonance spectrum of mixtures of nuclear spin-polarized noble gases and vapors of spin-polarized alkali-metal atoms. *Phys. Rev. A*, 39:5613–5623, Jun 1989.
- [24] T. G. Walker and W. Happer. Spin-exchange optical pumping of noble-gas nuclei. *Rev. Mod. Phys.*, 69:629–642, Apr 1997.
- [25] E. B. Aleksandrov, A. A. Ansel’m, Yu. V. Pavlov, and R. M. Umarchodzhaev. A restriction on the existence of a new type of fundamental interaction (the ”arion” long-range interaction) in an experiment on spin precession of mercury nuclei. *Sov. Phys. JETP*, 58:1103, Dec 1983.
- [26] B. J. Venema, P. K. Majumder, S. K. Lamoreaux, B. R. Heckel, and E. N. Fortson. Search for a coupling of the earth’s gravitational field to nuclear spins in atomic mercury. *Phys. Rev. Lett.*, 68:135–138, Jan 1992.

- [27] S. K. Lamoreaux, J. P. Jacobs, B. R. Heckel, F. J. Raab, and N. Fortson. New constraints on time-reversal asymmetry from a search for a permanent electric dipole moment of ^{199}Hg . *Phys. Rev. Lett.*, 59:2275–2278, Nov 1987.
- [28] J. P. Jacobs, W. M. Klipstein, S. K. Lamoreaux, B. R. Heckel, and E. N. Fortson. Testing time-reversal symmetry using ^{199}Hg . *Phys. Rev. Lett.*, 71:3782–3785, Dec 1993.
- [29] J. P. Jacobs, W. M. Klipstein, S. K. Lamoreaux, B. R. Heckel, and E. N. Fortson. Limit on the electric-dipole moment of ^{199}Hg using synchronous optical pumping. *Phys. Rev. A*, 52:3521–3540, Nov 1995.
- [30] M. V. Romalis, W. C. Griffith, J. P. Jacobs, and E. N. Fortson. New limit on the permanent electric dipole moment of ^{199}Hg . *Phys. Rev. Lett.*, 86:2505–2508, Mar 2001.
- [31] W. C. Griffith, M. D. Swallows, T. H. Loftus, M. V. Romalis, B. R. Heckel, et al. Improved limit on the permanent electric dipole moment of ^{199}Hg . *Phys. Rev. Lett.*, 102:101601, Mar 2009.
- [32] S. K. Peck, D. K. Kim, D. Stein, D. Orbaker, A. Foss, et al. Limits on local lorentz invariance in mercury and cesium. *Phys. Rev. A*, 86:012109, Jul 2012.
- [33] A. N. Youdin, D. Krause, Jr., K. Jagannathan, L. R. Hunter, and S. K. Lamoreaux. Limits on spin-mass couplings within the axion window. *Phys. Rev. Lett.*, 77:2170–2173, Sep 1996.
- [34] Larry Hunter, Joel Gordon, Stephen Peck, Daniel Ang, and Jung-Fu Lin. Using the earth as a polarized electron source to search for long-range spin-spin interactions. *Science*, 339(6122):928–932, 2013.
- [35] L. R. Hunter and D. G. Ang. Using geoelectrons to search for velocity-dependent spin-spin interactions. *Phys. Rev. Lett.*, 112:091803, Mar 2014.
- [36] T. E. Chupp, E. R. Oteiza, J. M. Richardson, and T. R. White. Precision frequency measurements with polarized ^3He , ^{21}Ne , and ^{129}Xe atoms. *Phys. Rev. A*, 38:3998–4003, Oct 1988.
- [37] T. E. Chupp, R. J. Hoare, R. L. Walsworth, and Bo Wu. Spin-exchange-pumped ^3He and ^{129}Xe zeeman masers. *Phys. Rev. Lett.*, 72:2363–2366, Apr 1994.
- [38] R. E. Stoner, M. A. Rosenberry, J. T. Wright, T. E. Chupp, E. R. Oteiza, et al. Demonstration of a two species noble gas maser. *Phys. Rev. Lett.*, 77:3971–3974, Nov 1996.
- [39] D. Bear, T. E. Chupp, K. Cooper, S. DeDeo, M. Rosenberry, et al. Improved frequency stability of the dual-noble-gas maser. *Phys. Rev. A*, 57:5006–5008, Jun 1998.
- [40] Mark A. Rosenberry. *A Precision Measurement of the ^{129}Xe Electric Dipole Moment Using Dual Noble Gas Masers*. PhD thesis, University of Michigan, 2000.
- [41] Alexander G. Glenday, Claire E. Cramer, David F. Phillips, and Ronald L. Walsworth. Limits on anomalous spin-spin couplings between neutrons. *Phys. Rev. Lett.*, 101:261801, Dec 2008.
- [42] M. Bulatowicz, R. Griffith, M. Larsen, J. Mirijanian, C. B. Fu, et al. Laboratory search for a long-range t -odd, p -odd interaction from axionlike particles using dual-species nuclear magnetic resonance with polarized ^{129}Xe and ^{131}Xe gas. *Phys. Rev. Lett.*, 111:102001, Sep 2013.
- [43] C. Gemmel, W. Heil, S. Karpuk, K. Lenz, Ch. Ludwig, et al. Ultra-sensitive magnetometry based on free precession of nuclear spins. *The European Physical Journal D*, 57(3):303–320, Apr 2010.
- [44] C. Gemmel, W. Heil, S. Karpuk, K. Lenz, Yu. Sobolev, et al. Limit on lorentz and cpt violation of the bound neutron using a free precession $^3\text{He}/^{129}\text{Xe}$ comagnetometer. *Phys. Rev. D*, 82:111901, Dec 2010.
- [45] K. Tullney, F. Allmendinger, M. Burghoff, W. Heil, S. Karpuk, et al. Constraints on Spin-Dependent Short-Range Interaction between Nucleons. *Physical Review Letters*, 111(10):100801, September 2013.
- [46] F. Allmendinger, I. Engin, W. Heil, S. Karpuk, H.-J. Krause, et al. Measurement of the permanent electric dipole moment of the ^{129}Xe atom. *Phys. Rev. A*, 100:022505, Aug 2019.
- [47] N. Sachdeva and I. Fan. New limit on the permanent electric dipole moment of ^{129}Xe using ^3He comagnetometry and squid detection.
- [48] T. W. Kornack and M. V. Romalis. Dynamics of two overlapping spin ensembles interacting by spin exchange. *Phys. Rev. Lett.*, 89:253002, Dec 2002.
- [49] T. W. Kornack, R. K. Ghosh, and M. V. Romalis. Nuclear spin gyroscope based on an atomic comagnetometer. *Phys. Rev. Lett.*, 95:230801, Nov 2005.
- [50] J. Lee, A. Almasi, and M. Romalis. Improved limits on spin-mass interactions. *Phys. Rev. Lett.*, 120:161801, Apr 2018.
- [51] Attaallah Almasi, Junyi Lee, Himawan Winarto, Marc Smiciklas, and Michael V. Romalis. New limits on anomalous spin-spin interactions. *Phys. Rev. Lett.*, 125:201802, Nov 2020.
- [52] M. Smiciklas, J. M. Brown, L. W. Cheuk, S. J. Smullin, and M. V. Romalis. New Test of Local Lorentz Invariance Using a ^{21}Ne -Rb-K Comagnetometer. *Physical Review Letters*, 107(17):171604, October 2011.
- [53] P. W. Graham, D. E. Kaplan, J. Mardon, S. Rajendran, W. A. Terrano, et al. Spin precession experiments for light axionic dark matter. *Phys. Rev. D*, 97:055006, Mar 2018.
- [54] Itay M. Bloch, Yonit Hochberg, Eric Kuflik, and Tomer Volansky. Axion-like relics: new constraints from old comagnetometer data. *Journal of High Energy Physics*, 2020(1):167, Jan 2020.

- [55] E. M. Purcell and N. F. Ramsey. On the possibility of electric dipole moments for elementary particles and nuclei. *Phys. Rev.*, 78:807–807, Jun 1950.
- [56] G. 't Hooft. Symmetry breaking through bell-jackiw anomalies. *Phys. Rev. Lett.*, 37:8–11, Jul 1976.
- [57] A. D. Sakharov. Violation of cp invariance, ? asymmetry, and baryon asymmetry of the universe. *Sov. Phys. JETP Lett.*, 5:24, Jul 1967.
- [58] T. G. Vold, F. J. Raab, B. Heckel, and E. N. Fortson. Search for a permanent electric dipole moment on the ^{129}Xe atom. *Phys. Rev. Lett.*, 52:2229–2232, Jun 1984.
- [59] Timothy Chupp and Michael Ramsey-Musolf. Electric dipole moments: A global analysis. *Phys. Rev. C*, 91:035502, Mar 2015.
- [60] L. I. Schiff. Measurability of nuclear electric dipole moments. *Phys. Rev.*, 132:2194–2200, Dec 1963.
- [61] V. V. Flambaum and J. S. M. Ginges. Nuclear schiff moment and time-invariance violation in atoms. *Phys. Rev. A*, 65:032113, Feb 2002.
- [62] Kota Yanase and Noritaka Shimizu. Large-scale shell-model calculations of nuclear schiff moments of ^{129}Xe and ^{199}Hg . *Phys. Rev. C*, 102:065502, Dec 2020.
- [63] Timo Fleig and Martin Jung. \mathcal{P}, \mathcal{T} -odd interactions in atomic ^{129}Xe and phenomenological applications. *Phys. Rev. A*, 103:012807, Jan 2021.
- [64] G. Cocconi and E. Salpeter. A search for anisotropy of inertia. *Il Nuovo Cimento (1955-1965)*, 10(4):646–651, Nov 1958.
- [65] Alan P. Lightman and David L. Lee. Restricted proof that the weak equivalence principle implies the einstein equivalence principle. *Phys. Rev. D*, 8:364–376, Jul 1973.
- [66] Sidney Coleman and Sheldon L. Glashow. Cosmic ray and neutrino tests of special relativity. *Physics Letters B*, 405(3):249–252, 1997.
- [67] Don Colladay and V. Alan Kostelecký. CPT violation and the standard model. *Phys. Rev. D*, 55:6760–6774, Jun 1997.
- [68] V. Alan Kostelecký and Charles D. Lane. Constraints on lorentz violation from clock-comparison experiments. *Phys. Rev. D*, 60:116010, Nov 1999.
- [69] O. W. Greenberg. *cpt* violation implies violation of lorentz invariance. *Phys. Rev. Lett.*, 89:231602, Nov 2002.
- [70] Nima Arkani-Hamed, Hsin-Chia Cheng, Markus Luty, and Jesse Thaler. Universal dynamics of spontaneous lorentz violation and a new spin-dependent inverse-square law force. *Journal of High Energy Physics*, 2005(07):029–029, jul 2005.
- [71] Mark P Haugan. Energy conservation and the principle of equivalence. *Annals of Physics*, 118(1):156–186, 1979.
- [72] Ch. Eisele, A. Yu. Nevsky, and S. Schiller. Laboratory test of the isotropy of light propagation at the 10^{-17} level. *Phys. Rev. Lett.*, 103:090401, Aug 2009.
- [73] V. V. Flambaum and M. V. Romalis. Limits on lorentz invariance violation from coulomb interactions in nuclei and atoms. *Phys. Rev. Lett.*, 118:142501, Apr 2017.
- [74] M. V. Romalis, D. Sheng, B. Saam, and T. G. Walker. Comment on “new limit on lorentz-invariance- and *cpt*-violating neutron spin interactions using a free-spin-precession ^3He – ^{129}Xe comagnetometer”. *Phys. Rev. Lett.*, 113:188901, Oct 2014.
- [75] F. Allmendinger, U. Schmidt, W. Heil, S. Karpuk, A. Scharth, et al. Allmendinger et al. reply:. *Phys. Rev. Lett.*, 113:188902, Oct 2014.
- [76] W. A. Terrano, J. Meinel, N. Sachdeva, T. E. Chupp, S. Degenkolb, et al. Frequency shifts in noble-gas comagnetometers. *Phys. Rev. A*, 100:012502, Jul 2019.
- [77] J. E. Moody and F. Wilczek. New macroscopic forces? *Phys. Rev. D*, 30:130–138, Jul 1984.
- [78] B. Arlen Young. Search for a gravity shift in the proton larmor frequency. *Phys. Rev. Lett.*, 22:1445–1446, Jun 1969.
- [79] D. J. Wineland, J. J. Bollinger, D. J. Heinzen, W. M. Itano, and M. G. Raizen. Search for anomalous spin-dependent forces using stored-ion spectroscopy. *Phys. Rev. Lett.*, 67:1735–1738, Sep 1991.
- [80] Bogdan A Dobrescu and Irina Mocioiu. Spin-dependent macroscopic forces from new particle exchange. *Journal of High Energy Physics*, 2006(11):005–005, nov 2006.
- [81] Pavel Fadeev, Yevgeny V. Stadnik, Filip Ficek, Mikhail G. Kozlov, Victor V. Flambaum, et al. Revisiting spin-dependent forces mediated by new bosons: Potentials in the coordinate-space representation for macroscopic- and atomic-scale experiments. *Phys. Rev. A*, 99:022113, Feb 2019.
- [82] Peter Vorob'ev and Igor' Kolokolov. DETECTORS FOR THE COSMIC AXIONIC WIND. *arXiv e-prints*, pages astro-ph/9501042, January 1995.
- [83] Peter W. Graham and Surjeet Rajendran. New observables for direct detection of axion dark matter. *Phys. Rev. D*, 88:035023, Aug 2013.
- [84] C. Abel, N. J. Ayres, G. Ban, G. Bison, K. Bodek, et al. Search for axionlike dark matter through nuclear spin precession in electric and magnetic fields. *Phys. Rev. X*, 7:041034, Nov 2017.

- [85] Teng Wu, John W. Blanchard, Gary P. Centers, Nataniel L. Figueroa, Antoine Garcon, et al. Search for axionlike dark matter with a liquid-state nuclear spin comagnetometer. *Phys. Rev. Lett.*, 122:191302, May 2019.
- [86] T. Braine, R. Cervantes, N. Crisosto, N. Du, S. Kimes, et al. Extended search for the invisible axion with the axion dark matter experiment. *Phys. Rev. Lett.*, 124:101303, Mar 2020.
- [87] Brent M. Graner. *Reduced Limit on the Permanent Electric Dipole Moment of ^{199}Hg* . PhD thesis, University of Washington, 2017.
- [88] S. F. Huelga, C. Macchiavello, T. Pellizzari, A. K. Ekert, M. B. Plenio, et al. Improvement of frequency standards with quantum entanglement. *Phys. Rev. Lett.*, 79:3865–3868, Nov 1997.
- [89] M. E. Limes, N. Dural, M. V. Romalis, E. L. Foley, T. W. Kornack, et al. Dipolar and scalar ^3He – ^{129}Xe frequency shifts in stemless cells. *Phys. Rev. A*, 100:010501, Jul 2019.
- [90] J. S. Waugh, L. M. Huber, and U. Haeberlen. Approach to high-resolution nmr in solids. *Phys. Rev. Lett.*, 20:180–182, Jan 1968.
- [91] K. U. Schreiber and JP. R. Wells. Invited review article: Large ring lasers for rotation sensing. *Review of Scientific Instruments*, 84(4):041101, 2013.
- [92] K. Ulrich Schreiber, Thomas Kluegel, and Geoffrey E. Stedman. Earth tide and tilt detection by a ring laser gyroscope. *Journal of Geophysical Research: Solid Earth*, 108(B2), 2003.
- [93] K. U. Schreiber, A. Velikoseltsev, M. Rothacher, T. Kluegel, G. E. Stedman, et al. Direct measurement of diurnal polar motion by ring laser gyroscopes. *Journal of Geophysical Research: Solid Earth*, 109(B6), 2004.
- [94] <https://jewellinstruments.com/products/geo/ultra-precision/600-series/model-a603/>.
- [95] H. B. Dang, A. C. Maloof, and M. V. Romalis. Ultrahigh sensitivity magnetic field and magnetization measurements with an atomic magnetometer. *Applied Physics Letters*, 97(15):151110, 2010.
- [96] D. Sheng, A. Kabcenell, and M. V. Romalis. New classes of systematic effects in gas spin comagnetometers. *Phys. Rev. Lett.*, 113:163002, Oct 2014.
- [97] M. E. Limes, D. Sheng, and M. V. Romalis. ^3He – ^{129}Xe comagnetometry using ^{87}Rb detection and decoupling. *Phys. Rev. Lett.*, 120:033401, Jan 2018.
- [98] A. Korver, D. Thrasher, M. Bulatowicz, and T. G. Walker. Synchronous spin-exchange optical pumping. *Phys. Rev. Lett.*, 115:253001, Dec 2015.
- [99] D. A. Thrasher, S. S. Sorensen, J. Weber, M. Bulatowicz, A. Korver, et al. Continuous comagnetometry using transversely polarized xe isotopes. *Phys. Rev. A*, 100:061403, Dec 2019.
- [100] Susan S. Sorensen, Daniel A. Thrasher, and Thad G. Walker. A synchronous spin-exchange optically pumped nmr-gyroscope. *Applied Sciences*, 10(20), 2020.
- [101] T. Sato, Y. Ichikawa, S. Kojima, C. Funayama, S. Tanaka, et al. Development of co-located ^{129}Xe and ^{131}Xe nuclear spin masers with external feedback scheme. *Physics Letters A*, 382(8):588–594, 2018.
- [102] Teng Wu, John W. Blanchard, Derek F. Jackson Kimball, Min Jiang, and Dmitry Budker. Nuclear-spin comagnetometer based on a liquid of identical molecules. *Phys. Rev. Lett.*, 121:023202, Jul 2018.
- [103] M. Pospelov, S. Pustelny, M. P. Ledbetter, D. F. Jackson Kimball, W. Gawlik, et al. Detecting domain walls of axionlike models using terrestrial experiments. *Phys. Rev. Lett.*, 110:021803, Jan 2013.
- [104] Samer Afach, Ben C. Buchler, Dmitry Budker, Conner Dailey, Andrei Derevianko, et al. Search for topological defect dark matter using the global network of optical magnetometers for exotic physics searches (gnome), 2021.